Emergence of film-thickness- and grain-size-dependent elastic properties in nanocrystalline thin films

Jie Lian,[a,1] Seok-Woo Lee,[a,1] Lorenzo Valdevit,[b] Michael I. Baskes[c] and Julia R. Greer[a,*]

[a]Division of Engineering and Applied Sciences, California Institute of Technology, 1200 East California Boulevard, MC 309-81, Pasadena, CA 91125-8100, USA
[b]Department of Mechanical and Aerospace Engineering, University of California, 4227 Engineering Gateway, Irvine, CA 92697-3975, USA
[c]Department of Mechanical and Aerospace Engineering, University of California, San Diego, 9500 Gilman Dr., La Jolla, CA 92093, USA

Molecular dynamics simulations of nanocrystalline Ni revealed that the in-plane Young's modulus of 2.2 nm grained Ni film with ∼10 grains across its thickness was only 0.64% smaller than that of bulk, while it dropped to 24.1% below bulk value for ∼1 grain across film. This size dependence arises from the increased number of more compliant grains adjacent to the free surface. Simulations of nanocrystalline diamond revealed that the anharmonicity of the potential curve determined the sensitivity of the Young's modulus to variations in the sample size.

Nanostructures, such as nanowires, nanobelts and nanofilms, often possess unique electrical, chemical and mechanical properties [1–4], paving the way for their applications in sensors, biological and biomedical devices, and microelectromechanical systems. For these applications, the device functionality directly depends on the structural robustness of the materials comprising them. Mechanical properties of nanostructures have been shown to deviate significantly from their bulk counterparts and, in many cases, unique mechanical behavior begins to emerge even if only one (as opposed to all) dimension is reduced to the nanoscale [5–9]. In addition to film thickness, grain size also influences mechanical properties of nanostructures, such as hardness, elastic modulus [10,11] and stress/strain response [12], especially in the nanometer regime. The combined effects of these nanodimensions – limited external dimensions (i.e. film thickness) and characteristic microstructural length scale (i.e. grain size) – likely have a significant effect on the elastic properties of thin films [13–15].

The Young's modulus is probably the single, most commonly used entity to characterize the elastic response of a solid. Multiple studies have been carried out to investigate the dependence of Young's modulus on the characteristic length scale of thin films and small-scale structures [16–24]. In all computational and theoretical work, the uncovered variation in the elastic constants, which are directly linked to the Young's modulus, with film thickness has been attributed to several factors. These include surface-stress-induced anisotropic lattice parameter changes [16,23,25], variations in the atomic structure caused by coupling between the in-plane contractions and subsequent yielding in the out-of-plane direction [26], different bond length variation driven by the crystallographic orientation of film's surface relative to the loading direction [5], and competition between atomic coordination and electron redistribution [24]. To date, most of the computational investigations of elastic properties of nanostructures have been focused on single crystals and could not capture the complex effects that might be caused by grain boundaries [5,20,22,24]. Few experimental studies on nanocrystalline, rather than single crystalline, films have reported the dependence of the Young's modulus on film thickness [27,28]. The existing experimental studies on the elastic deformation of

---

*Corresponding author. Tel.: +1 626 396 4127; e-mail: jrgreer@caltech.edu
[1] The first two authors contributed equally to the work.

nanocrystalline thin films are limited, and fundamental deformation mechanisms that lead to the observed size dependence remain unclear. This work aims at filling this knowledge gap by performing a systematic numerical investigation of the effect of grain size and film thickness on elastic properties of nanocrystalline Ni and diamond.

This investigation of the effect of combined intrinsic and extrinsic dimensional limitations on elastic modulus is further motivated by the development of ultralight cellular microtrusses, which consist of periodically organized nanocrystalline Ni–P hollow tubes connected at the nodes, which have been shown to exhibit unique mechanical properties, including full recovery from ~50% compression with significant energy absorption [29]. Experimental and numerical investigations revealed that these ultralight materials were buckling dominated at relative densities lower than ~0.2% [30]. The critical buckling strength is proportional to the elastic modulus – which further underlines the importance of quantifying the Young's modulus as a function of wall thickness and of grain size for each material.

We utilized molecular dynamics (MD) simulations to investigate the grain size dependence of bulk and Young's moduli of nanocrystalline Ni, for grain sizes between 2.2 and 10.5 nm. We further explored the relationship between the in-plane elastic modulus of nanocrystalline Ni thin films with 2.2 nm grain sizes and a range of film thickness, systematically varying from 3.6 nm (~1 grain across) to 35.2 nm (~10 grains across). Finite elements simulations of the elastic response of Ni thin films were conducted to assess the possible effects of crystallographic texture and to separate continuum vs. atomistic effects. To understand the underlying physics of the sensitivity of the Young's modulus to both film thickness and grain size, the elastic properties of nanocrystalline diamond with grain sizes of 1.5 and 3 nm were also determined. Diamond has a fundamentally different bonding nature, which causes its interatomic potential to be substantially different from that of Ni. The relationship between the Young's modulus and the shape of the potential curve was carefully examined.

Bulk and thin film nanocrystalline Ni samples with randomly oriented grains, whose size ranged from 2.2 to 10.5 nm, were created and placed on a face-centered cubic lattice (Fig. 1).

Details for calculating elastic constants and bulk modulus are provided in the Supplementary Information. To study the effect of film thickness on the Young's modulus, computational blocks with grain sizes of 2.2 nm and film thicknesses of ~1, 2, 3, 5 and 10 grains in height were created. Five samples with different configurations of randomly oriented grains were constructed for each film thickness, and the average Young's modulus was calculated to account for the possible effects of crystallographic texture when such a small number of grains were present. The NPT ensemble at 300 K and 0 GPa in all three dimensions was applied to the sample for 50 ps to achieve equilibrium before mechanical tests. Periodic boundary conditions were applied along the in-plane directions, and zero-traction conditions were imposed in the z-direction (Fig. 1). Incremental tensile strains were applied in the x-direction at a rate of $\dot{\varepsilon} = 1.0 \times 10^6 s^{-1}$ at 300 K, and zero pressure was maintained in the y-direction to al-
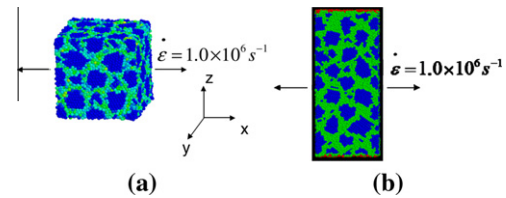

Figure 1. (a) Simulation cell of bulk nanocrystalline Ni subjected to tension at a strain rate of $1.0 \times 10^6 s^{-1}$; (b) simulation cell of nanocrystalline Ni film with five grains across its thickness (z-direction) subjected to tension at a strain rate of $1.0 \times 10^6 s^{-1}$. Atoms are colored using the centrosymmetry parameter [31], with the dark blue atoms having a bulk face-centered cubic environment and the lighter colored atoms a grain boundary environment. (For interpretation of the references to colour in this figure legend, the reader is referred to the web version of this article.)

low for Poisson's contraction. The resulting stress state of the computational block was $\sigma_y = \sigma_z = 0$ and $\sigma_x = \varepsilon \cdot E$. The Young's modulus was calculated by fitting the slope of tensile stress–strain data between 0 and 0.007 strains.

We used an identical computational methodology to investigate the elastic attributes of nanocrystalline diamond films with different grain sizes. To calculate the Young's modulus of bulk and thin-film nanocrystalline diamond, two different methods were used: (M1) the stress–strain curve method, identical to the procedure used for nanocrystalline Ni; and (M2) a long-time NPT method. In M1, the Young's modulus was determined by linearly fitting the loading portion of the stress–strain curve, generated at a strain rate of 10^9 s^{-1}, between the strains of 0 and 0.1. This strain rate, which was three orders of magnitude higher than for nanocrystalline Ni, was chosen because of the lengthy computational times for diamond. It is unlikely that the Young's modulus is sensitive to strain rates between 10^6 and 10^9 s^{-1}. The long-time NPT method (M2) measured the time-averaged strain at two points: −600 and 600 MPa, or ~10^{-3} strain. This small strain ensured that deformation was restricted to being nearly pure elastic. The Young's modulus was then interpolated from the slope of the line connecting stress–strain points at −600 and 600 MPa.

To compare the Young's modulus of nanocrystalline Ni and diamond as a function of grain size and film thickness, both parameters were normalized by the equilibrium first neighbor distance (Fig. 2). The Young's modulus of nanocrystalline Ni decreased by 41.5%, from 174.5 to 117.1 GPa, with grain size reduction from 10.5 to 2.2 nm (see Supplementary Information). This suggests that smaller-grained samples may exhibit higher compressibility, likely due to the higher volume fraction of grain boundaries, where interatomic bonds are more compliant as compared with the grain interior. Young's moduli of nanocrystalline Ni films with thicknesses of ~10 grains were close to the macroscale Young's modulus, while the one-grain-thick samples exhibited an ~24.1% reduction in Young's modulus as compared with the bulk (see Supplementary Information). Compared to nanocrystalline Ni, the effects of both the grain size and the film thickness were much weaker for the nanocrystalline diamond than for the nanocrystalline Ni. Young's modulus of nanocrystalline Ni decreased by 13% with the reduction of normalized grain size from
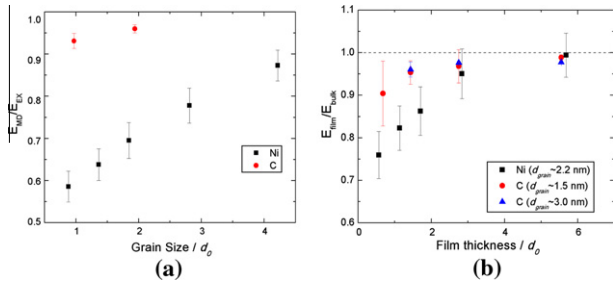
Figure 2. (a) Young's modulus of bulk nanocrystalline Ni and diamond, normalized by the coarse-grained value (E_{EX}) as a function of normalized grain size; d (b) Young's modulus of nanocrystalline thin film, normalized by the bulk nanocrystalline value as a function of normalized film thickness. Here, the grain size and film thickness are both normalized by the appropriate equilibrium first neighbor distance, $d_0^{Ni} = 2.489 \dot{A}$ and $d_0^c = 1.545 \dot{A}$.

~2 to 1, while that of nanocrystalline diamond diminished by only 2%. Similarly, the reduction in normalized film thickness by a factor of 6 resulted in a 30% drop in the Young's modulus in Ni and by less than 10% in diamond for both grain sizes.

To ascertain whether any continuum effects could be partly responsible for the observed size effect, finite elements simulations of thin films with 1–20 grains across the thickness were performed and resulted in no discernible size effect (see Supplementary Information). This implies that the strong dependence of the Young's modulus on film thickness brought to light by MD simulations is not a continuum effect and is likely due entirely to the surface effects.

To understand the possible differences in the Young's modulus of the grain interior vs. the grain boundaries in bulk nanocrystalline Ni, we first calculated these quantities as:

$$E_{GB} = \frac{1}{N_{GB} \cdot \Omega_m} \frac{\sum_{i=1}^{N_{GB}} \sigma_{ixx}}{\varepsilon_{xx}} ; E_{GI} = \frac{1}{N_{GI} \cdot \Omega_m} \frac{\sum_{i=1}^{N_{GI}} \sigma_{ixx}}{\varepsilon_{xx}} \quad (1)$$

where N_{GB} and N_{GI} are the total numbers of each type of atoms, Ω_m is the equilibrium volume per atom, and σ_{ixx} and ε_{xx} are the stress·volume per atom and strain in the loading direction (in LAMMPS, σ_{ixx} is in units of stress·volume). The centrosymmetry parameter method was used to differentiate grain boundary atoms from grain interior ones [31]. Atoms with centrosymmetry parameter $P < 1$ were defined as grain interior, and $P > 1$ corresponded to grain boundary. Figure 3(a) shows Young's modulus of these two types of atoms as a function of grain size in bulk nanocrystalline Ni in one sample test. This plot reveals that Young's moduli of the grain interior became insensitive to grain size beyond ~3.4 nm, remaining at 167.5 ± 3.0 GPa. In smaller-grained samples ($d = 2.2$ nm), the modulus was ~20% lower than that, at 135 GPa. The average Young's modulus of the grain boundary region remained nearly constant, at 103.1 ± 6.8 GPa, for all grain sizes considered. This suggests that grain boundaries are more compliant than internal grains, a finding that is consistent with the notion that samples with a larger volume fraction of grain boundary atoms are more compliant.

To explore the origins of the film-thickness-dependent Young's modulus, we examined Young's moduli of grain
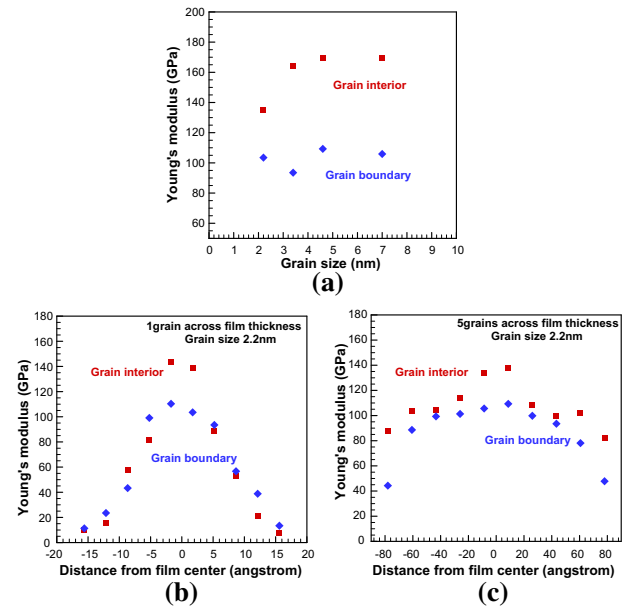
Figure 3. (a) Young's modulus of grain interior region and grain boundary region vs. grain size in bulk nanocrystalline Ni; Young's modulus of grain interior region and grain boundary region in nanocrystalline Ni thin film vs. distance from the film center: (b) one grain across the film thickness; (c) five grains across the film thickness.

interior and of grain boundaries as a function of their proximity to the surface. The Young's modulus of each atomic layer was calculated by following the same methodology as applied to bulk nanocrystalline sample. Results are plotted as a function of the distance from the mid-thickness point (Fig. 3b and c) for samples with a single grain across thickness (3.6 nm thick film) and five grains across thickness (17.3 nm thick film). For the former, the average modulus of the grain interior close to the surface was 8.8 ± 1.7 GPa, which is 90.1% lower than the average value. The Young's modulus of the grain interior atoms gradually increased to 140.9 ± 3.4 GPa in the center of the film. Similarly, the Young's modulus of the grain boundary atoms gradually increased from 12.4 ± 1.5 GPa in the surface region to 106.9 ± 4.8 GPa at the film center. For thicker films, the surface modulus of grain interior atoms was 84.8 ± 3.9 GPa, which is 23.7% lower than that of the film, and slightly increased to 135.6 ± 2.9 GPa in the center. Figure 3 clearly indicates that the observed gradient in the modulus for both interior grains and grain boundaries is limited to the ~1 grain wide surface (~2 nm); as a result, the average modulus quickly approached the bulk value for thicker films.

Surface effects on the Young's modulus of thin films can be summarized as follows:
(1) No size effects were observed for the Young's modulus in the bulk of thin films.
(2) Dependence of the Young's modulus on the film thickness in nanocrystalline Ni films was attributed to surface effects, with the surface modulus being 90.1% lower than that within the film (for both the grain interior and the grain boundary).
(3) Thicker films had higher surface moduli, likely because of the lower relative fraction of unsaturated bonds, which intensifies bonding between surface atoms.

(4) The influence of the surface becomes less pronounced in thicker films.

Surface stress has previously been shown to be the major reason for the thickness dependence of the Young's modulus in thin films [32]. Surface stress is related to surface energy variation with respect to applied strain, therefore different potential curves would be expected to dictate distinct film thickness dependences of Young's modulus. Dingreville et al. [32] demonstrated that the thickness dependence of the Young's modulus was related to the magnitude of the third-order elastic constants, with the apparent Young's modulus calculated as:

$$E_{apparent} = E_{bulk} + \frac{1}{a} f(C_{ij}, C_{ijk}) \qquad (2)$$

where $E_{apparent}$ is the thickness-dependent Young's modulus, E_{bulk} is the Young's modulus of the bulk form, a is half of the film thickness, and C_{ij} and C_{ijk} are second- and third-order elastic constants. This model is in good agreement with MD simulations for a free-standing Cu thin film for Young's modulus calculations. The non-vanishing third-order elastic constants are also correlated with the extent of anharmonicity of the potential energy curve, since $C_{ijk} = 0$ for a completely harmonic potential curve. Hence, the larger anharmonicity of Ni compared with diamond is consistent with a more pronounced size effect (Fig. 2).

In summary, we performed MD simulations to investigate the elastic properties of nanocrystalline Ni in bulk and of nanocrystalline Ni and diamond in thin film geometries. The Young's modulus of nanocrystalline Ni was found to decrease from 174.5 to 117.1 GPa when the grain size was systematically reduced from 10.5 to 2.2 nm. Reduction of the specimen geometry to thin films also affected the elastic properties: the Young's modulus decreased from 116.3 to 88.9 GPa when the film thickness was reduced from 35.2 nm (∼10 grains across height) to 3.6 nm (∼1 grain across height). We demonstrated that this reduction in Young's modulus with decreasing film thickness could not be explained by a continuum framework; rather, it is likely attributed to "surface effects", i.e. a substantial reduction in the modulus in the surface atomic planes.

The elastic properties of nanocrystalline diamond with grain sizes of 1.5 and 3 nm were compared with those of nanocrystalline Ni. Diamond has substantially different bonding energetics, which causes its interatomic potential to exhibit a significant amount of anharmonicity (i.e. asymmetry). While the Young's modulus of nanocrystalline Ni decreased by 13% with a twofold reduction in the normalized grain size, the modulus of nanocrystalline diamond diminished by only 2%. Similarly, a sixfold reduction in the normalized film thickness resulted in a 30% drop in the Young's modulus in Ni and a less than 10% drop in diamond for both grain sizes. These results correlate well with the marked difference in the anharmonicity of the interatomic potential shape, and suggest that the sensitivity of the Young's modulus to grain size and film thickness may stem from the degree of harmonicity in the potential energy curve: a greater degree of anharmonicity amplifies their effects.

[1] A.N. Belov, S.A. Gavrilov, V.I. Shevyakov, in: Proceedings of the International Conference on Nanomeeting, 2007, pp. 447.
[2] H.G. Craighead, Science 290 (2000) 1532.
[3] K.S. Shankar, A.K. Raychaudhuri, Mater. Sci. Eng. C-Bio. S. 25 (2005) 738.
[4] Y.N. Xia, P.D. Yang, Y.G. Sun, Y.Y. Wu, B. Mayers, B. Gates, Y.D. Yin, F. Kim, Y.Q. Yan, Adv. Mater. 15 (2003) 353.
[5] G.X. Cao, X. Chen, Int. J. Solids Struct. 45 (2008) 1730.
[6] S. Cuenot, C. Fretigny, S. Demoustier-Champagne, B. Nysten, Phys. Rev. B 69 (2004) 165410-1.
[7] X.X. Li, T. Ono, Y.L. Wang, M. Esashi, Appl. Phys. Lett. 83 (2003) 3081.
[8] S.G. Nilsson, X. Borrise, L. Montelius, Appl. Phys. Lett. 85 (2004) 3555.
[9] E.W. Wong, P.E. Sheehan, C.M. Lieber, Science 277 (1997) 1971.
[10] Z.H. Cao, P.Y. Li, H.M. Lu, Y.L. Huang, X.K. Meng, J. Phys. D: Appl. Phys. 42 (2009) 065405.
[11] M. Wiora, K. Brühne, A. Flöter, P. Gluche, T.M. Willey, S.O. Kucheyev, A.W. Van Buuren, A.V. Hamza, J. Biener, H.-J. Fecht, Diamond Relat. Mater. 18 (2009) 927.
[12] R. Venkatraman, J.C. Bravman, J. Mater. Res. 7 (2011) 2040.
[13] E. Arzt, Acta Mater. 46 (1998) 5611.
[14] J.R. Greer, J.T.M. De Hosson, Prog. Mater. Sci. 56 (2011) 654.
[15] O. Kraft, P.A. Gruber, R. Monig, D. Weygand, Annu. Rev. Mater. Res. 40 (2011) 293.
[16] R.C. Cammarata, K. Sieradzki, Phys. Rev. Lett. 62 (1989) 2005.
[17] R. Dingreville, A.J. Kulkarni, M. Zhou, J.M. Qu, Model. Simul. Mater. Sci. 16 (2008) 025002-1.
[18] W. Kim, M. Cho, Model. Simul. Mater. Sci. 18 (2010) 085006-1.
[19] X.H. Liang, B. Wang, Y.L. Liu, Int. J. Solids Struct. 46 (2009) 322.
[20] S.S. Liu, Y.H. Wen, Z.Z. Zhu, Chin. Phys. B 17 (2008) 2621.
[21] R.E. Miller, V.B. Shenoy, Nanotechnology 11 (2000) 139.
[22] V.B. Shenoy, Phys. Rev. B 71 (2005) 094104-1.
[23] F.H. Streitz, R.C. Cammarata, K. Sieradzki, Phys. Rev. B 49 (1994) 10699.
[24] L.G. Zhou, H.C. Huang, Appl. Phys. Lett. 84 (2004) 1940.
[25] D. Wolf, J.F. Lutsko, Phys. Rev. Lett. 60 (1988) 1170.
[26] D. Wolf, Appl. Phys. Lett. 58 (1991) 2081.
[27] V. Chawla, R. Jayaganthan, R. Chandra, B Mater. Sci. 32 (2009) 117.
[28] G. Guisbiers, E. Herth, L. Buchaillot, T. Pardoen, Appl. Phys. Lett. 97 (2010) 143115.
[29] T.A. Schaedler, A.J. Jacobsen, A. Torrents, A.E. Sorensen, J. Lian, J.R. Greer, L. Valdevit, W.B. Carter, Science 334 (2011) 962.
[30] A. Torrents, T.A. Schaedler, A.J. Jacobsen, W.B. Carter, L. Valdevit, Acta Mater. 60 (2012) 3511.
[31] C.L. Kelchner, S.J. Plimpton, J.C. Hamilton, Phys. Rev. B 58 (1998) 11085.
[32] R. Dingreville, J. Qu, C. Mohammed, J. Mech. Phys. Solids 53 (2005) 1827.